Phase Transitions, Crystal Structures, and Magnetic Properties of Ferrocenium Ionic Plastic Crystals with CF3BF3 and Other Anions

Kimata, Hironori
Sakurai, Takahiro
Ohta, Hitoshi
Mochida, Tomoyuki

(Citation)
ChemistrySelect,4(4):1410-1415

(Issue Date)
2019-01-31

(Resource Type)
journal article

(Version)
Accepted Manuscript

Phase Transitions, Crystal Structures, and Magnetic Properties of Ferrocenium Ionic Plastic Crystals with CF_3BF_3 and Other Anions

Hironori Kimata,[a] Takahiro Sakurai,[b] Hitoshi Ohta,[c,d] and Tomoyuki Mochida*[a]

[a] *Prof. Dr. T. Mochida, H. Kimata*
Department of Chemistry, Graduate School of Science, Kobe University, Rokkodai, Nada, Hyogo 657-8501 (Japan)
E-mail: tmochida@platinum.kobe-u.ac.jp
[b] *Dr. T. Sakurai*
Research Facility Center for Science and Technology, Kobe University, Rokkodai, Nada, Hyogo 657-8501 (Japan)
[c] *Prof. Dr. H. Ohta*
Molecular Photoscience Research Center, Kobe University, Rokkodai, Nada, Hyogo 657-8501 (Japan)
[d] *Prof. Dr. H. Ohta*
Department of Physics, Graduate School of Science, Kobe University, Rokkodai, Nada, Hyogo 657-8501 (Japan)
Supporting information for this article is available on the WWW under http://

Abstract: Salts of cationic sandwich complexes often exhibit an ionic plastic phase; however, only a few exhibit a plastic phase at room temperature. To explore the use of the CF_3BF_3 anion to lower the transition temperature to the plastic phase, we prepared salts of CF_3BF_3 with various ferrocene derivatives, [D][CF_3BF_3] (D = FeCp*$_2$, Fe(C_5Me_4H)$_2$, Fe(C_5H_4Me)$_2$, FeCp(C_5H_4Me), FeCp$_2$; Cp* = C_5Me_5, Cp = C_5H_5). Although [FeCp*$_2$][CF_3BF_3] exhibited a plastic phase above 417 K, the other salts formed room-temperature ionic plastic crystals with a phase transition to the plastic phase in the range 266–291 K. The crystal structure and thermal properties of [FeCp$_2$][OTf] were elucidated for comparison. In addition, decamethylferrocenium salts with other anions were synthesized and structurally characterized: [FeCp*$_2$]X (X = N(SO_2F)$_2$ and B(CN)$_4$) exhibited a phase transition to the plastic phase above 400 K, whereas carborane-containing salts [FeCp*$_2$]$_2$[$B_{12}F_{12}$] and [FeCp*$_2$][Co($C_2B_9H_{11}$)$_2$] did not exhibit a plastic phase.

Introduction

Recently, ionic plastic crystals containing onium cations have attracted significant attention for their potential use in solid electrolytes.[1] A plastic phase is a highly disordered phase exhibited by solids of globular molecules, in which their orientations are disordered while their centroids are ordered in the crystal lattice.[2] Ionic crystals that exhibit a plastic phase are called ionic plastic crystals and have attracted research interest owing to their ionic conductivity. Many salts containing sandwich complexes exhibit a plastic phase because of their nearly spherical molecular shape;[3] however, the temperature of the phase transition (T_C) to the plastic phase is generally high, and only a few salts are known to exhibit a plastic phase at room temperature.[4] In the pursuit of a molecular design to lower the transition temperature, we developed various ionic plastic crystals containing cationic sandwich complexes and investigated the correlation between molecular size and transition temperature.[4–8] By investigating diamagnetic salts containing Co or Ru, we found that CF_3BF_3 is a useful anion that lowers the transition temperature.[8] Accordingly, in this study, we synthesized salts of ferrocene derivatives with CF_3BF_3 to explore room-temperature paramagnetic ionic plastic crystals, which are intriguing research targets.[5,9] The CF_3BF_3 anion is known to produce ionic liquids and ionic plastic crystals.[10]

This paper reports the thermal properties, crystal structures, and magnetic properties of ferrocene-based salts containing CF_3BF_3 and other anions (Figure 1). We synthesized CF_3BF_3 salts with various cations, [D][CF_3BF_3] (D = $FeCp^*_2$ (**1**), $Fe(C_5Me_4H)_2$ (**2**), $Fe(C_5H_4Me)_2$ (**3**), $FeCp(C_5H_4Me)$ (**4**), $FeCp_2$; Cp* = C_5Me_5, Cp = C_5H_5). In addition, we synthesized decamethylferrocenium salts with other anions, [**1**][X] (X = FSA, $B(CN)_4^-$, $Co(C_2B_9H_{11})_2^-$) and [**1**]$_2$[$B_{12}F_{12}$]. Moreover, the crystal structure and phase transitions of [$FeCp_2$][OTf] (OTf = $CF_3SO_3^-$) were elucidated for comparison with those of [$FeCp_2$][CF_3BF_3]. The phase transitions in these salts are discussed in comparison with those of the related salts.

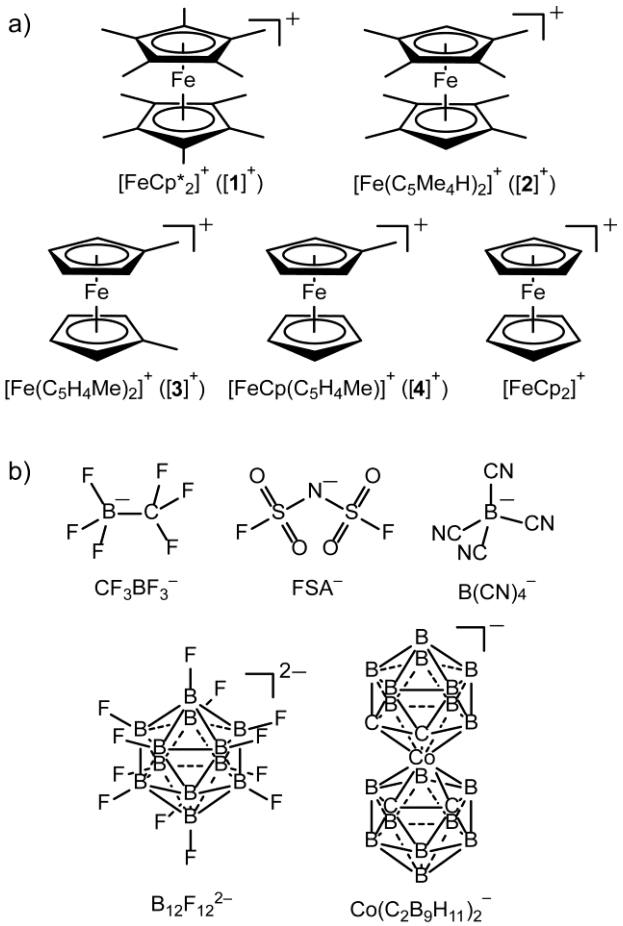

Figure 1. Structural formulae of the (a) cationic sandwich complexes and (b) anions used in this study.

Results and Discussion

Phase transition to a plastic phase

The salts were prepared from the corresponding chloride salts by anion exchange. The phase transitions in these salts were investigated using differential scanning calorimetry (DSC) (Figure S1, Supporting Information). All salts, except for the carborane-containing salts ([**1**][$Co(C_2B_9H_{11})_2$] and [**1**]$_2$[$B_{12}F_{12}$]), exhibited a transition to a plastic phase. The phase sequences of these salts are shown in Figure 2. Several salts exhibited additional phase transitions, as has been reported for other ferrocene-containing salts,[4] which may be related to the order/disorder of the anion.

All the CF_3BF_3 salts exhibited a plastic phase at room temperature except for [**1**][CF_3BF_3], which exhibited a plastic phase above 416.9 K (Figure 2a). The T_C values of [**2**][CF_3BF_3], [**3**][CF_3BF_3], [**4**][CF_3BF_3], and [**5**][CF_3BF_3] were ~270, 265.6, 291.3, and 270.4 K, respectively. Despite the almost

identical shapes and volumes of the anions, the T_C of $[FeCp_2][CF_3BF_3]$ (270.4 K) was considerably lower than that of $[FeCp_2][OTf]$ (338.5 K; Figure 2b). The phase transition of **[2]**$[CF_3BF_3]$ (T_C = ~270 K) was unusual because it occurred over a wide temperature range (250–300 K) regardless of the scan rate (5–40 K min^{-1}). In addition, sample-dependence was observed: Samples with higher crystallinity exhibited the transition at lower temperatures, whereas powdered samples exhibited no DSC peak due to broadening of the transition. These phenomena, which were confirmed by polarization microscopy observations (Figure S2, Supporting Information), are ascribed to an inhomogeneous phase transition in the crystal.

[1]$[N(SO_2F)_2]$ and **[1]**$[B(CN)_4]$ exhibited high T_C values of 446.8 and 410.8 K, respectively (Figure 2c). In contrast, carborane-containing salts (**[1]**$[Co(C_2B_9H_{11})_2]$ and **[1]**$_2[B_{12}F_{12}]$) exhibited no phase transitions, which was attributed to the elongated shape of the anion or stronger electrostatic interactions in the divalent salt.

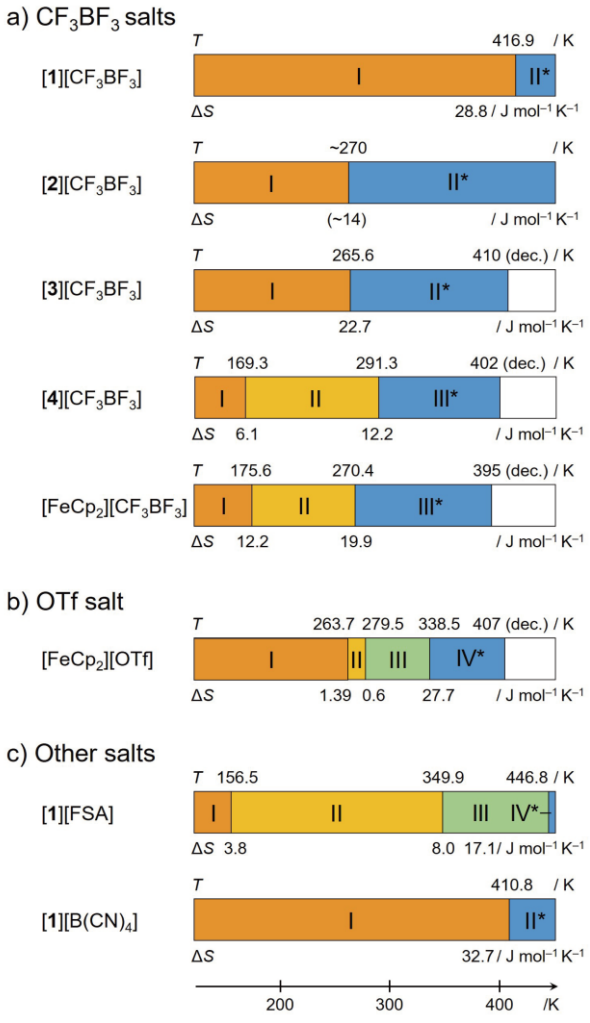

Figure 2. Phase sequences of the salts investigated in this study. The phase transition temperature (K) and transition entropy (J mol^{-1} K^{-1}) of each phase transition are shown above and below the bar charts, respectively. The asterisks indicate the plastic phases.

Comparison of transition temperatures

As shown in the previous section, the investigated CF_3BF_3 salts were room-temperature ionic plastic crystals that transitioned to the plastic phase below 300 K, except for [**1**][CF_3BF_3]. [**1**][X] (X = PF_6, CF_3BF_3, OTf) generally exhibited high transition temperatures. In this section, their phase transition temperatures are discussed in comparison with those of related salts.

The phase transition temperatures of [$FeCp_2$][X] and [$CoCp_2$][X], some of which were obtained from the literature,[3a,8,11] are summarized in Figure 3a. It is evident that the two series exhibit similar tendencies: The transition temperatures of the CF_3BF_3 salts are ~90 K lower than those of the OTf salts, as was also observed for [$RuCp(C_6H_6)$][X].[8] The higher transition temperatures of the OTf salts are likely due to charge localization on the oxygen atom in the anion, leading to stronger electrostatic interactions in the crystal. The phase sequences of [$FeCp_2$][X] (X = CF_3BF_3, OTf; Figure 2) were more complicated than those of the corresponding [$CoCp_2$] salts,[8] i.e., they exhibited an additional phase transition, despite there being only a slight difference in the molecular volumes of the cations ($[FeCp_2]^+$: 169.1 $Å^3$ and $[CoCp_2]^+$: 166.9 $Å^3$).

The phase transition temperatures of [**1**][X] and [**2**][X] are shown in Figure 3b along with the data for the BF_4, PF_6, OTf, and Tf_2N salts.[4] The phase transition temperatures of [**2**][X] are ~100 K lower than those of [**1**][X] with the same anion. In addition, the phase transition temperature tends to decrease with increasing anion size; the exception being that salts with the unsymmetrical FSA anion exhibit relatively high transition temperatures. As discussed previously, a plausible explanation for the overall tendency is that the contacts between the cations get larger with decreasing radius ratio ($\rho = r_{\text{small ion}}/r_{\text{large ion}}$), suppressing the molecular rotation due to steric hindrance of the methyl groups, which probably led to the increase in the transition temperature.[5] In contrast to the case of [MCp_2][X]

(M = Fe, Co) discussed above, the transition temperatures of the CF_3BF_3 and OTf salts were comparable in [**1**][X] ([**1**][CF_3BF_3]: T_C = 416.9 K, [**1**][OTf]: 419.7 K[4]) and [**2**][X] ([**2**][CF_3BF_3]: T_C = ~270 K, [**2**][OTf]: T_C = 288.6 K[4]). This is ascribed to $[\mathbf{1}]^+$ and $[\mathbf{2}]^+$ having considerably larger cation volumes (351.3 and 315.7 Å^3, respectively) than $[MCp_2]^+$, which reduces the influence of the local charge distribution in the anion on the cation–anion electrostatic interactions.

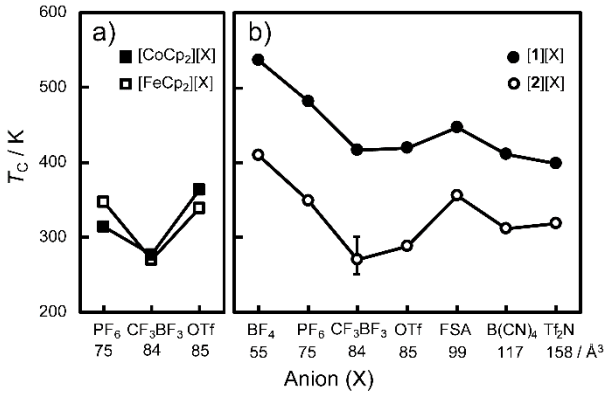

Figure 3. Phase transition temperatures to the plastic phase of (a) $[FeCp_2][X]$ and $[CoCp_2][X]$ and (b) [**1**][X] and [**2**][X]. The data for salts other than those examined in this study were obtained from the literature.[3a,8,11] The phase transition of [**2**][CF_3BF_3] occurs over a wide temperature range. The van der Waals volumes (Å^3)[8] of each anion are provided below the charts.

Structures of the plastic phase

The structures of the plastic phases of the CF_3BF_3 salts at room temperature were investigated by powder X-ray diffraction (PXRD) measurements (Figure S3, Supporting Information). The analysis showed that [**2**][CF_3BF_3] and [**3**][CF_3BF_3] have *anti*-NiAs-type structures, whereas [**4**][CF_3BF_3] and $[FeCp_2][CF_3BF_3]$ have the CsCl-type structures. We previously reported that [**2**][$B(CN)_4$] and [**2**][$C(CN)_3$] also have the *anti*-NiAs-type structures,[5] though ionic plastic crystals having the *anti*-NiAs-type structure are only few.[1c]

The lattice constants and interionic distances derived from the PXRD data are shown in Table 1. The radii of $[\mathbf{2}]^+$, $[\mathbf{3}]^+$, $[\mathbf{4}]^+$ and $[FeCp_2]^+$ estimated from the van der Waals volumes assuming the

molecule to be a sphere were 4.22, 3.66, 3.55 and 3.43 Å, respectively, whereas the radii of $CF_3BF_3^-$ was 2.71 Å. The interionic distances were found to be comparable to the sum of the ionic radii (Table 1). According to the radius ratio rule for inorganic ionic crystals,[13] a salt with a radius ratio ($\rho = r_{anion}/r_{cation}$) greater than 0.73 exhibits a CsCl-type structure with coordination number eight, whereas a salt with a radius ratio between 0.41–0.73 exhibits a NaCl- or (*anti*-)NiAs-type structure with coordination number six. The radius ratios for [**2**][CF_3BF_3] and [**3**][CF_3BF_3], having the *anti*-NiAs-type structure, were 0.64 and 0.74, respectively, whereas those for [**4**][CF_3BF_3] and [$FeCp_2$][CF_3BF_3], having the CsCl-type structure, were 0.76 and 0.79, respectively. Therefore, the radius ratio rule holds. The deviation of [**2**][CF_3BF_3] having the *anti*-NiAs-type structure despite ρ = 0.74 (> 0.73) is probably due to limited accuracy in estimation of the molecular radii.

Table 1. Lattice constants, interionic distances, and radius ratio in the plastic phase

	Structure type	Lattice constant (Å)	Interionic distances (Å)		Radius ratio[a]
			Experimental	Calculated[b]	Calculated
[**2**][CF_3BF_3]	*anti*-NiAs	$a = b = 8.62$, $c = 13.10$	6.62	6.94	0.64
[**3**][CF_3BF_3]	*anti*-NiAs	$a = b = 7.83$, $c = 12.50$	6.15	6.38	0.74
[**4**][CF_3BF_3]	CsCl	7.02	6.08	6.26	0.76
[$FeCp_2$][CF_3BF_3]	CsCl	6.79	5.88	6.14	0.79

[a]Value of r_{anion}/r_{cation}, where the ionic radii are calculated from molecular volumes determined by DFT calculations. [b]Sum of the calculated radii of the cation and anion.

Magnetic properties

The temperature dependence of the magnetic susceptibilities of [$FeCp_2$][CF_3BF_3] (T_C = 270.4 K), [**2**][CF_3BF_3] (T_C = ~270 K), and [**3**][CF_3BF_3] (T_C = 265.6 K) are shown in Figure 4 in the form of χT–T plots. The χT values of these salts at 273 K were in the range 0.51–0.67 emu K mol^{-1}. These values correspond to the magnetic susceptibility of the ferrocenium cation.[14] The salts exhibited simple paramagnetic behaviors down to low temperatures. The magnetic moments of [$FeCp_2$][CF_3BF_3] and [**3**][CF_3BF_3] decreased gradually below 100 K, which was likely because of the loss of the orbital contribution.[14]

The magnetic susceptibility of $[FeCp_2][CF_3BF_3]$ exhibited a slight change (~0.07 emu K mol^{-1}) at the phase transitions between phase I and phase II (~170 K) and between phase II and the plastic phase (~270 K), each phase transition featuring hysteresis. However, [**2**][CF_3BF_3] and [**3**][CF_3BF_3] exhibited no magnetic susceptibility changes at the phase transition temperatures. All the salts exhibited only negligible field dependence (0.1–5 T) of the magnetic susceptibilities, similar to the case of [**2**][MCl_4] (M = Fe, Ga[5]). Therefore, the application of magnetic fields had no observable orientation effect in the present salts, although the orientation of plastic crystals can be controlled by electronic fields.[15] This is possibly due to the absence of effective magnetic anisotropy in the low-temperature phase. A magnetic-field orientation effect during the liquid–solid phase transition has been observed in an ionic liquid containing a ferrocenium cation.[16]

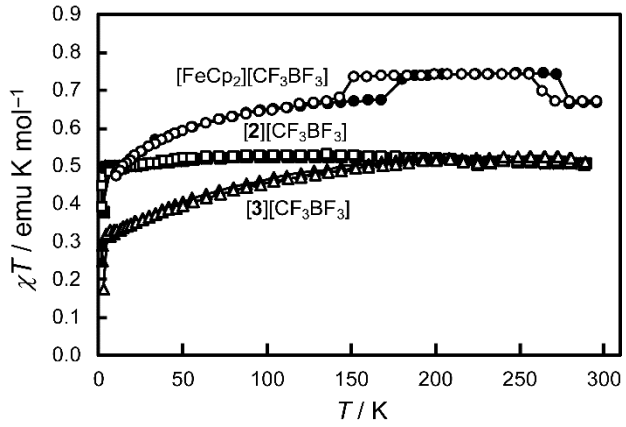

Figure 4. Temperature dependence of the magnetic susceptibilities (χT–T plots) of $[FeCp_2][CF_3BF_3]$, [**2**][CF_3BF_3], and [**3**][CF_3BF_3] measured under a 1 T magnetic field. The cooling and heating data are indicated by open and filled symbols, respectively.

Low-temperature structures

The crystal structures of phase I (i.e., the lowest temperature phase) of [**1**][X] (X = CF_3BF_3, FSA, $B(CN)_4$, $Co(C_2B_9H_{11})_2$) and $[\mathbf{1}]_2[B_{12}F_{12}]$ were determined at 100 K. The anions and cations were alternately arranged in these salts. In addition, the structure of $[FeCp_2][OTf]$ in phase I was determined at 90 K. The ORTEP diagrams of the cations and anions in these salts are shown in Figure

S4 (Supporting Information). Attempts at the structural determination of the salts that exhibit a plastic phase at room temperature were unsuccessful.

The packing diagrams of [**1**][X] (X = CF_3BF_3, FSA, $B(CN)_4$) are shown in Figure 5. In these crystals, six anions surround each cation and *vice versa*; hence, their structures have a coordination number of six,[12] which is consistent with their radius ratios (0.62–0.69). With respect to the cation orientation, each unit cell of these salts contains two types of cations that are oriented with their C_5 axes almost perpendicular to each other. The salts of **1** and **2** often exhibit unidirectional alignment of the cations in the crystal;[4,5,17] therefore, the present salts are exceptional. In [**1**][CF_3BF_3] (space group *P*nnm, $Z = 2$), the carbon and boron atoms in the anion are disordered (0.5:0.5). The molecular arrangement of this crystal is almost identical with that of [**1**][OTf] in phase II, although [**1**][OTf] has a lower symmetry space group ($Pmn2_1$) owing to the absence of anion disorder.[17] Their structural similarity may contribute to their comparable phase transition temperatures. Another difference is that [**1**][OTf] exhibits rotational disorder of the Cp* ring.[17] The structures of [**1**][FSA] (space group *C*2/c, $Z = 12$) and [**1**][$B(CN)_4$] (space group $P3_221$, $Z = 3$) differ from those of [**2**][FSA] (space group $Pca2_1$) and [**2**][$B(CN)_4$] (space group $I4_1/acd$),[5] which exhibit unidirectional alignment of the cations in the crystal. One of the two independent anions in [**1**][FSA] exhibits rotational disorder (Figure S4, Supporting Information).

The packing diagrams of the carborane-containing salts are shown in Figure 6. The crystal of [**1**][$Co(C_2B_9H_{11})_2$] (space group $P2_1/n$, $Z = 4$) is isomorphous with that of [**1**][$M(C_2B_9H_{11})_2$] (M = Fe, Ni)[18], and the C_5 axes of the cations are aligned parallel to the *a*-axis (Figure 5a). On the other hand, [**1**]$_2$[$B_{12}F_{12}$] is a divalent salt (space group $P2_1/n$, $Z = 4$) with the unit cell containing eight cations and four anions (Figure 5b). In the crystal, two anions are surrounded by fourteen cations. The C_5 axes of the cations are not aligned unidirectionally. There are short contacts between the ring carbons of the cation and fluorine atoms of the anion (C···F = 2.940, 2.970 Å); these values are 0.2 Å shorter than the combined van der Waals radii. The geometry of the anion is comparable to those of cobaltocene salts or a ferrocene derivative with the $B_{12}F_{12}$ anion.[19] Preliminary X-ray measurements

revealed that the salts of **2** with these anions are isomorphous with the salts of **1**.

The structure of $[FeCp_2][OTf]$ (space group $P2_1/c$, $Z = 12$) is isomorphous with that of $[CoCp_2][OTf]$.[20] The packing diagram of this salt is shown in Figure S5 (Supporting Information). The coordination number is eight, and the radius ratio is 0.80; hence, this structure is in agreement with the radius rule, which predicts a coordination number of eight for radius ratios greater than 0.73.

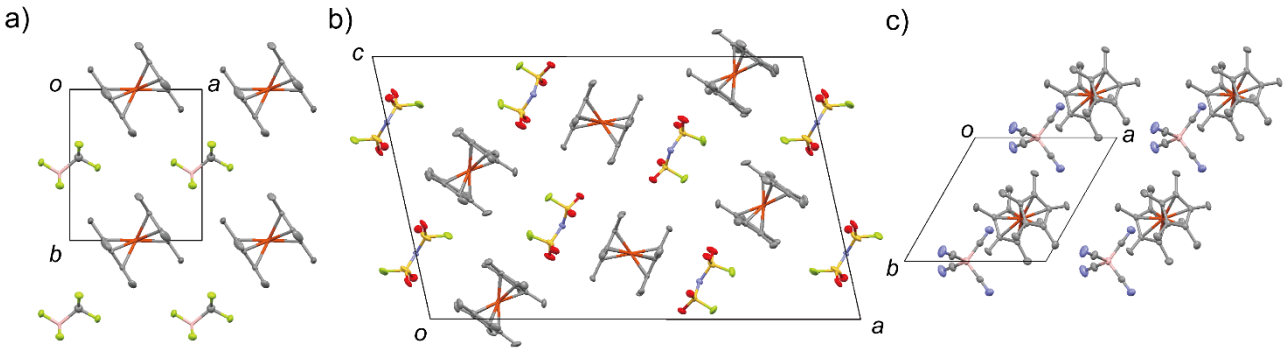

Figure 5. (a) Packing diagrams of [**1**][CF_3BF_3], (b) [**1**][FSA], and (c) [**1**][$B(CN)_4$]. Hydrogen atoms have been omitted for clarity.

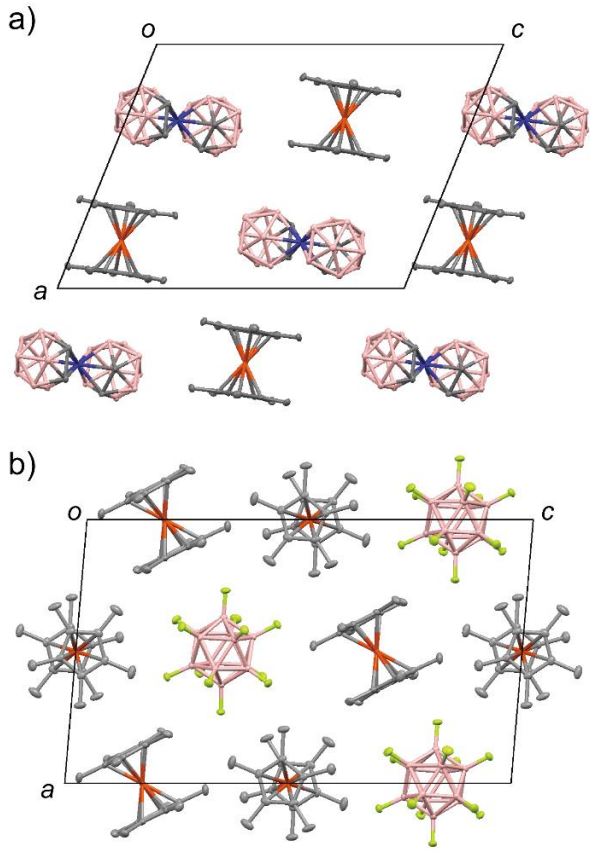

Figure 6. (a) Packing diagrams of [**1**][$Co(C_2B_9H_{11})_2$] and (b) [**1**]$_2$[$B_{12}F_{12}$]. Hydrogen atoms have been omitted for clarity.

Conclusion

We examined the phase transitions of salts of ferrocene derivatives with CF_3BF_3 and other anions. Only a few organometallic room-temperature ionic plastic crystals have been reported; however, most of the CF_3BF_3 salts synthesized in this study exhibited an ionic plastic phase at room temperature, demonstrating the effectiveness of the CF_3BF_3 anion. The ferrocenium salt with CF_3BF_3 exhibited a considerably lower phase transition temperature than that with OTf, although the transition temperatures of deca- or octamethylferrocenium salts containing CF_3BF_3 and OTf were comparable. The decamethylferrocenium salts prepared in this study exhibited plastic phases at high temperatures (> 400 K) except for the salts with carborane-related anions, which did not exhibit a plastic phase.

These salts exhibited paramagnetic behaviors with a slight or no magnetic susceptibility change during the phase transition. Further research is required on other ferrocenium salts to investigate the possibility of magnetic-field orientation.

Supporting Information Summary

Experimental details, DSC traces (Figure S1), POM images of [**2**][CF_3BF_3] (Figure S2), powder X-ray diffraction patterns (Figure S3), ORTEP drawings of the cations and anions (Figure S4), packing diagram of [$FeCp_2$][OTf] (Figure S5), and crystallographic parameters (Tables S1 and S2). CCDC-1850223 ([**1**][CF_3BF_3]), -1861515 ([**1**][FSA]), -1859202 ([**1**][$B(CN)_4$]), -1861514 ([**1**][$Co(C_2B_9H_{11})_2$]), -1863460 ([**1**]$_2$[$B_{12}F_{12}$]) and 1062864 ([$FeCp_2$][OTf]) contain the supplementary crystallographic data for this paper.

Acknowledgements

We thank Dr. Yusuke Funasako (Sanyo-Onoda City University) and Shingo Saruta (Toho University)

for their help with the preparation and X-ray structure analysis of [$FeCp_2$][OTf]. This work was financially supported by KAKENHI (grant number 16H04132) from the Japan Society for the Promotion of Science (JSPS).

Keywords: ionic plastic crystals, sandwich complexes, phase transitions, crystal structures, thermal properties

REFERENCES

[1] a) D. R. MacFarlane, J. Huang, M. Forsyth, *Nature* **1999**, *402*, 792–794; b) J. M. Pringle, *Phys. Chem. Chem. Phys.* **2013**, *15*, 1339–1351; c) K. Matsumoto, U. Harinaga, R. Tanaka, A. Koyama, R. Hagiwara, K. Tsunashima, *Phys. Chem. Chem. Phys.* **2014**, *16*, 23616–23626; d) Y. Abu-Lebdeh, P.-J. Alarco, M. Armand, *Angew. Chem. Int. Ed.* **2003**, *42*, 4499–4501; *Angew. Chem.* **2003**, *115*, 4637–4639; e) Z. B. Zhou, H. Matsumoto, *Electrochem. Commun.* **2007**, *9*, 1017–1022; f) J. Luo, A. H. Jensen, N. R. Brooks, J. Sniekers, M. Knipper, D. Aili, Q. Li, B. Vanroy, M. Webbenhorst, F. Yan, L. V. Meervelt, Z. Shao, J. Fang, Z.-H. Luo, D. E. De Vos, K. Binnemans, J. Fransaer, *Energy Environ. Sci.* **2015**, *8*, 1276–1291; g) M. Lee, U. H. Choi, S. Wi, C. Slebodnick, R. H. Colby, H. W. Gibson, *J. Mater. Chem.* **2011**, *21*, 12280–12287.

[2] a) J. Timmermans, *J. Phys. Chem. Solids* **1961**, *18*, 1–8; b) J. Sherwood, *The Plastically Crystalline State: Orientationally Disordered Crystals*, Wiley, Chichester, **1979**.

[3] a) R. J. Webb, M. D. Lowery, Y. Shiomi, M. Sorai, R. J. Wittebort D. N. Hendrickson, *Inorg. Chem.* **1992**, *31*, 5211–5219; b) D. Braga, F. Paganelli, E. Tagliavini, S. Casolari, G. Cojazzi F. Grepioni, *Organometallics* **1999**, *18*, 4191–4196; c) H. Schottenberger, K. Wurst, U. J. Griesser, R. K. R. Jetti, G. Laus, R. H. Herber, I. Nowik, *J. Am. Chem. Soc.* **2005**, *127*, 6795–6801.

[4] T. Mochida, Y. Funasako, M. Ishida, S. Saruta, T. Kosone, T. Kitazawa, *Chem. Eur. J.* **2016**, *22*, 15725–15732.

[5] T. Mochida, M. Ishida, T. Tominaga, K. Takahashi, T. Sakurai, H. Ohta, *Phys. Chem. Chem. Phys.* **2018**, *20*, 3019–3028.

[6] T. Mochida, Y. Funasako, T. Inagaki, M. J. Li, K. Asahara, D. Kuwahara, *Chem. Eur. J.* **2013**, *19*, 6257–6264.

[7] T. Tominaga, T. Ueda, T. Mochida, *Phys. Chem. Chem. Phys*. **2017**, *19*, 4352–4359.

[8] H. Kimata, T. Mochida, *Cryst. Growth Des.*, DOI: 10.1021/acs.cgd.8b01390.

[9] I. de Pedro, A. García-Saiz, J. A. González, I. Ruiz de Larramendi, T. Rojo, C. Afonso, S. Simeonov, J. C.

Waerenborgh, J. A. Blanco, B. Ramajo J. Rodríguez, *Phys. Chem. Chem. Phys.* **2013**, *15,* 12724–12733.

[10] a) Z.-B. Zhou, H. Matsumoto, K. Tatsumi, *Chem. Lett.* **2004**, *33*, 1636–1637; b) Z.-B. Zhou, H. Matsumoto, K. Tatsumi, *Chem Eur. J.* **2005**, *11*, 752–766.

[11] F. Grepioni, G. Cojazzi, S. M. Draper, N. Scully, D. Braga, *Organometallics* **1998**, *17*, 296–307.

[12] D. M. Mingos, A. L. Rohl, *J. Chem. Soc. Dalton trans.* **1991**, 3419–3425.

[13] P. Atkins, T. Overton, J. Rourke, M. Weller, F. Armstrong, *Shriver and Atkins' Inorganic Chemistry*, Oxford University Press, Oxford, **2010**.

[14] D. N. Hendrickson, Y. S. Sohn, H. B. Gray, *Inorg. Chem.* **1971**, *10*, 1559–1563.

[15] J. Harada, T. Shimojo, H. Oyamaguchi, H. Hasegawa, Y. Takahashi, K. Satomi, Y. Suzuki, J. Kawamata, T. Inabe, *Nat. Chem.* **2016**, *11*, 1–7.

[16] Y. Funasako, T. Mochida, T. Inagaki, T. Sakurai, H. Ohta, K. Furukara, T. Nakamura, *Chem. Commun.* **2011**, *47*, 4475–4477.

[17] S. Hamada, Y. Funasako, T. Mochida, D. Kuwahara, K. Yoza, *J. Organomet. Chem.* **2012**, *713*, 35–41.

[18] a) J. M. Forward, D. M. P. Mingos, A. V. Powell, *J. Organomet. Chem.* **1994**, *465*, 251–258; b) J. D. McKinney, F. S. McQuillan, H. Chen, T. A. Hamor, C. J. Jones, M. Slaski, G. H. Cross, C. J. Harding, *J. Organomet. Chem.* **1997**, *547*, 253–262.

[19] a) M. Malischewski, E. V. Bukovsky, S. H. Strauss, K. Seppelt, *Inorg. Chem.* **2015**, *54*, 11563−11566; b) E. V. Bukovsky, M. R. Lacroix, N. J. DeWeerd, B. J. Reeves, Y. Kobayashi, M. B. Bayless, G. P. Bradshaw, Y. L. Choi, B. S. Newell, S. H. Strauss, *J. Organomet. Chem.* **2018**, *865*, 128–137.

[20] C. G. Andrews, C. L. B. Macdonald, *Acta Crystallogr. Sect. E* **2005**, *61*, m2103–m2105.

TOC

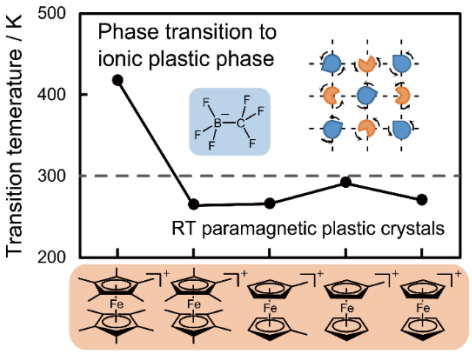

Room-temperature magnetic ionic plastic crystals. Phase transitions, crystal structures, and magnetic properties of salts of ferrocene derivatives with CF_3BF_3 and other anions were investigated. Most of the CF_3BF_3 salts exhibited a plastic phase at room temperature.

CONTENTS

Experimental

General

$[FeCp_2]Cl$[1] and $[FeCp_2][OTf]$[2] were prepared according to literature methods. $[FeCp(C_5H_4Me)]Cl$ was prepared according to the same method using methylferrocene in place of ferrocene (yield 11%). Other chemicals were commercially available. DSC measurements were performed using a TA Instruments Q100 differential scanning calorimeter at a rate of 10 K min^{-1}; other rates were applied as required. The decomposition temperatures were determined based on visual inspection with a microscope equipped with a heating stage. Infrared spectra were recorded via attenuated total reflectance (ATR; diamond) using a Thermo Scientific Nicolet iS-5 FT-IR spectrometer. Magnetic susceptibilities were measured using a Quantum Design MPMS-XL instrument under a 1 T magnetic field, which was varied between 0.1 and 5 T, as required. Powder XRD measurements were performed using Rigaku SmartLab. The van der Waals volumes and ionic radii of the molecules were estimated based on density functional theory calculations (B3LYP/LanL2DZ) using Spartan '18 (Wavefunction, Inc.).

Syntheses

$[FeCp^*_2][CF_3BF_3]$ ($[1][CF_3BF_3]$). Under a nitrogen atmosphere, SO_2Cl_2 (0.032 mL, 0.39 mmol) was added dropwise to a dichloromethane solution (0.3 mL) of $[FeCp^*_2]$ (85 mg, 0.21 mmol) with stirring. After 15 min, the solvent was evaporated under reduced pressure, and the residue was dried under vacuum. The obtained dark green solid was dissolved in water (0.5 mL), and an aqueous solution (0.2 mL) of $K[CF_3BF_3]$ (51 mg, 0.29 mmol) was added. After stirring for 15 min, dark-green precipitates were collected by filtration and washed with diethyl ether. Recrystallization of the product from acetone–diethyl ether (–40 °C) gave dark-green block crystals (55.7 mg, yield 79%). Anal. Calcd. for $C_{21}H_{30}F_6BFe$: C, 54.47; H, 6.53; N, 0.00. Found: C, 54.35; H, 6.72; N, 0.03. IR (cm^{-1}): 1478, 1427, 1383, 1114, 1093, 1045, 969, 944, 632, 533.

$[Fe(C_5Me_4H)_2][CF_3BF_3]$ ($[2][CF_3BF_3]$). This salt was prepared following the same procedure described for [**1**]$[CF_3BF_3]$ using $[Fe(C_5Me_4H)_2]$ (77 mg, 0.26 mmol), SO_2Cl_2 (0.033 mL, 0.42 mmol), and $K[CF_3BF_3]$ (68 mg, 0.42 mmol). The product was obtained as dark-green microcrystals (45.5 mg, yield 41%). Anal. Calcd. for $C_{19}H_{26}F_6BFe$: C, 52.45; H, 6.02; N, 0.00. Found: C, 51.99; H, 6.03; N, 0.00. IR (cm^{-1}):1455, 1385, 1112, 1095, 1050, 972, 947, 633.

$[Fe(C_5H_4Me)_2][CF_3BF_3]$ ($[3][CF_3BF_3]$). Under a nitrogen atmosphere, SO_2Cl_2 (0.080 mL, 0.98 mmol) was added to a dichloromethane solution (0.1 mL) of dimethylferrocene (130 mg, 0.61 mmol), and the solution was stirred for 15 min at 0 °C. The solvent was evaporated under reduced pressure, water (0.1 mL) was added, and the solution was filtered. An aqueous solution (0.2 mL) of $K[CF_3BF_3]$ (76 mg, 0.44 mmol) was added to the filtrate, and the solution was stirred for 10 min. The aqueous solution was removed by decantation, and the resultant blue residue was washed with diethyl ether. After drying under vacuum, slow diffusion of diethyl ether into an acetone solution of the solid for two days at –40 °C resulted in the precipitation of dark-blue crystals of the desired product, which was collected by filtration and dried under vacuum (28.8 mg, yield 14%). Anal. Calcd. for $C_{13}H_{14}F_6BFe$: C, 44.50; H, 4.02; N, 0.00. Found: C, 44.37; H, 4.22; N, 0.00. IR (cm^{-1}):1481, 1456, 1042, 975, 950, 851, 633.

[FeCp(C$_5$H$_4$Me)][CF$_3$BF$_3$] ([4][CF$_3$BF$_3$]). This salt was prepared following the same procedure described for [**3**][CF_3BF_3] using methylferrocene (142 mg, 0.71 mmol), SO_2Cl_2 (0.09 mL, 1.1 mmol), and K[CF_3BF_3] (99 mg, 0.53 mmol). The product was obtained as dark-blue crystals (24.3 mg, yield 10%) by slow diffusion of hexane into a dichloromethane solution. Anal. Calcd. for $C_{12}H_{12}F_6BFe$: C, 42.78; H, 3.59; N, 0.00. Found: C, 42.95; H, 3.62; N, 0.03. IR (cm^{-1}): 3119, 1480, 1420, 1041, 975, 949, 852, 633, 532.

[FeCp$_2$][CF$_3$BF$_3$]. Under a nitrogen atmosphere, an aqueous solution (0.2 mL) of K[CF_3BF_3] (77 mg, 0.44 mmol) was added to an aqueous solution (0.3 mL) of [$FeCp_2$]Cl (50 mg, 0.23 mmol), and the solution was stirred for 1 h. The resultant dark-blue precipitates were collected by filtration and washed with diethyl ether. The residue was dried under vacuum, dissolved in dichloromethane, and filtered. Slow diffusion of hexane into the dichloromethane solution over four days at −6 °C resulted in the precipitation of dark-blue needle crystals of the desired product, which was collected by filtration and dried under vacuum (24.2 mg, yield 33%). Anal. Calcd. for $C_{11}H_{10}F_6BFe$: C, 40.92; H, 3.12; N, 0.00. Found: C, 40.99; H, 3.02; N, 0.07. IR (cm^{-1}): 3120, 1419, 1040, 975, 948, 854, 632.

[FeCp*$_2$][FSA] ([1][FSA]). This salt was prepared following the same procedure described for [**1**][CF_3BF_3] using [$FeCp^*_2$] (53 mg, 0.16 mmol), SO_2Cl_2 (0.032 ml, 0.39 mmol), and K[FSA] (72 mg, 0.33 mmol). The product was obtained as dark-green block crystals (55.7 mg, yield 68%). Anal. Calcd. for $C_{20}H_{30}NF_2OSFe$: C, 47.43; H, 5.97; N, 2.77. Found: C, 47.27; H, 6.02; N, 2.74. IR (cm^{-1}): 1479, 1361, 1216, 1175(SO), 1102, 1022, 822, 732, 566, 536.

[Fe(Cp*)$_2$][B(CN)$_4$] ([1][B(CN)$_4$]). This salt was prepared following the same procedure described for [**1**][CF_3BF_3] using [$FeCp^*_2$] (51 mg, 0.15 mmol), SO_2Cl_2 (0.025 mL, 0.31 mmol), and K[$B(CN)_4$] (45 mg, 0.29 mmol). The product was obtained as dark-green block crystals (34.6 mg, yield 51%). Anal. Calcd. for $C_{24}H_{30}N_4BFe$: C, 65.34; H, 6.85; N, 12.70. Found: C, 65.20; H, 6.95; N, 12.54. IR (cm^{-1}): 1479, 1426, 1386, 1026, 930, 534.

[FeCp*$_2$][Co(C$_2$B$_9$H$_{11}$)$_2$] ([1][Co(C$_2$B$_9$H$_{11}$)$_2$]). This salt was prepared following the same procedure described for [**1**][CF_3BF_3] using [$FeCp^*_2$] (51 mg, 0.15 mmol), SO_2Cl_2 (0.019 mL, 0.24 mmol), and Na[$Co(C_2B_9H_{11})_2$] (50 mg, 0.14 mmol). Recrystallization of the product from acetonitrile (−40 °C) gave the product as green or orange needle crystals (11.7 mg, yield 12%). Anal. Calcd. for $C_{24}H_{52}B_{18}FeCo$: C, 44.34; H, 8.06; N, 0.00. Found: C, 44.19; H, 7.91; N, 0.00. IR (cm^{-1}): 2544, 1474, 1381, 1095, 1017, 977, 884, 721.

[FeCp*$_2$]$_2$[B$_{12}$F$_{12}$] ([1]$_2$[B$_{12}$F$_{12}$]). This salt was prepared following the same procedure described for [**1**][$Co(C_2B_9H_{11})_2$] using [$FeCp^*_2$] (42 mg, 0.13 mmol), SO_2Cl_2 (0.020 mL, 0.26 mmol), and $Cs_2[B_{12}F_{12}]$ (20 mg, 0.032 mmol). Recrystallization of the solid from acetone (−40 °C) gave the product as dark-green block crystals (13.5 mg, yield 42%). Anal. Calcd. for $C_{40}H_{60}B_{12}F_{12}Fe_2$: C, 47.55; H, 5.99; N, 0.00. Found: C, 47.30; H, 5.65; N, 0.00. IR (cm^{-1}):1381, 1217, 1018, 723.

X-Ray crystallography

Single crystals of [**1**]$_2$[$B_{12}F_{12}$] suitable for X-ray crystallography were obtained by slow evaporation of a methanol solution. Single crystals of the other salts were obtained as described above. Single crystal XRD data were collected at 100 K using a Bruker APEX II Ultra CCD diffractometer with MoKα radiation (λ = 0.71073

Å). The structures were determined by the direct method using SHELXL.[3] The crystallographic parameters are shown in **Tables S1** and **S2**.

References

[1] J. J. Adams, N. Arulsamy, B. P. Sullivan, D. M. Roddick, A. Neuberger, R. H. Schmehv, *Inorg. Chem*. **2015**, *54*, 11136–11149.

[2] R. R. Schrock, L. G. Sturgeoff, P. R. Sharp, *Inorg. Chem.* **1983**, *22*, 2801–2806.

[3] G. M. Sheldrick, *Acta Crystallogr.* **2008**, *A64*, 112–122.

(a) [**1**][CF_3BF_3]

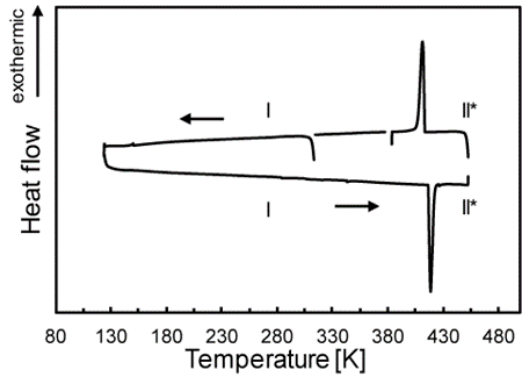

(b) [**2**][CF_3BF_3]

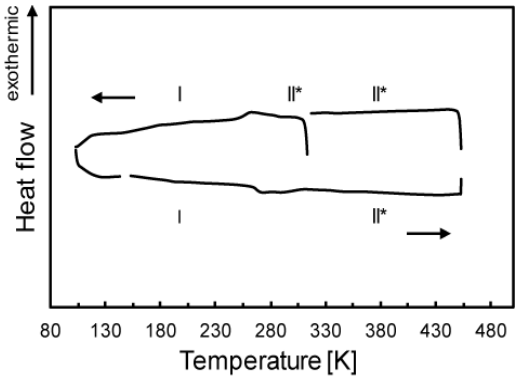

(c) [**3**][CF_3BF_3]

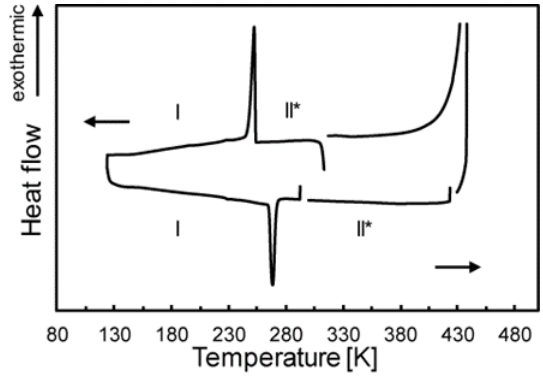

(d) [**4**][CF_3BF_3]

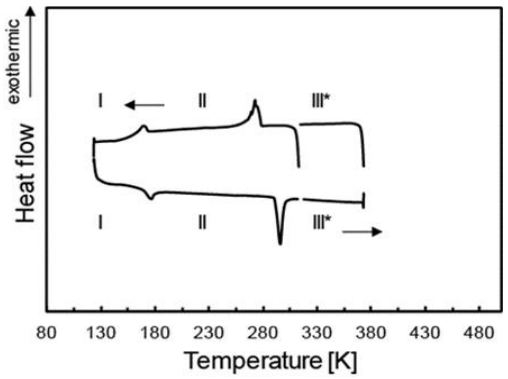

(e) [$FeCp_2$][CF_3BF_3]

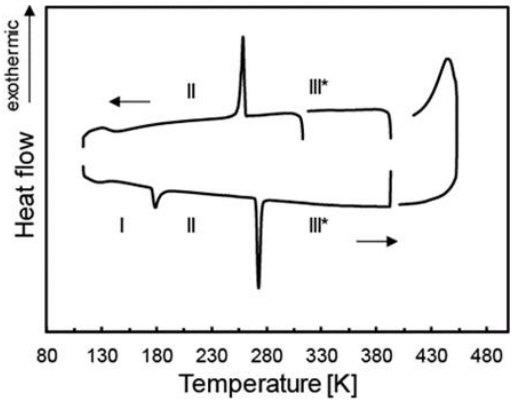

(f) [**1**][FSA]

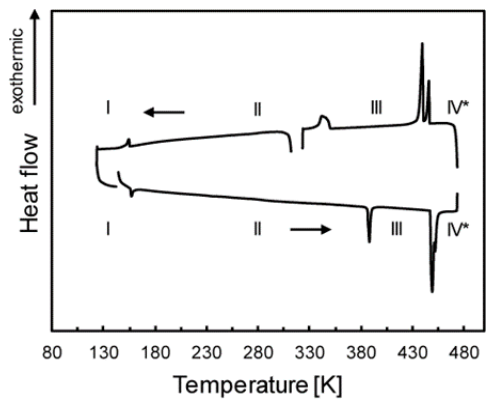

(g) [**1**][$B(CN)_4$]

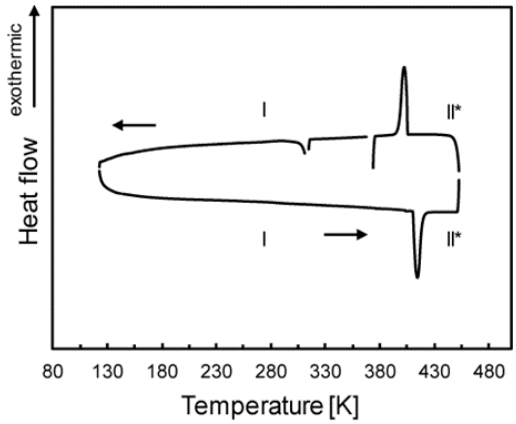

(h) [$FeCp_2$][OTf]

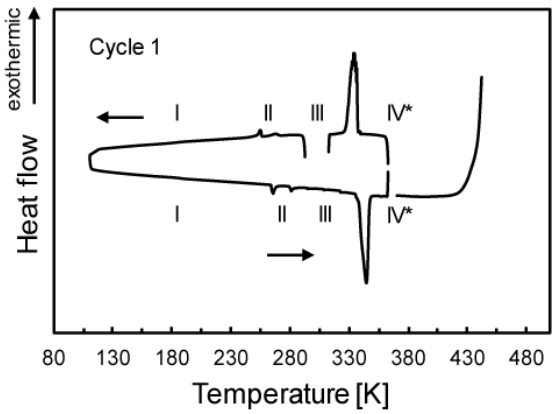

Figure S1. DSC traces.

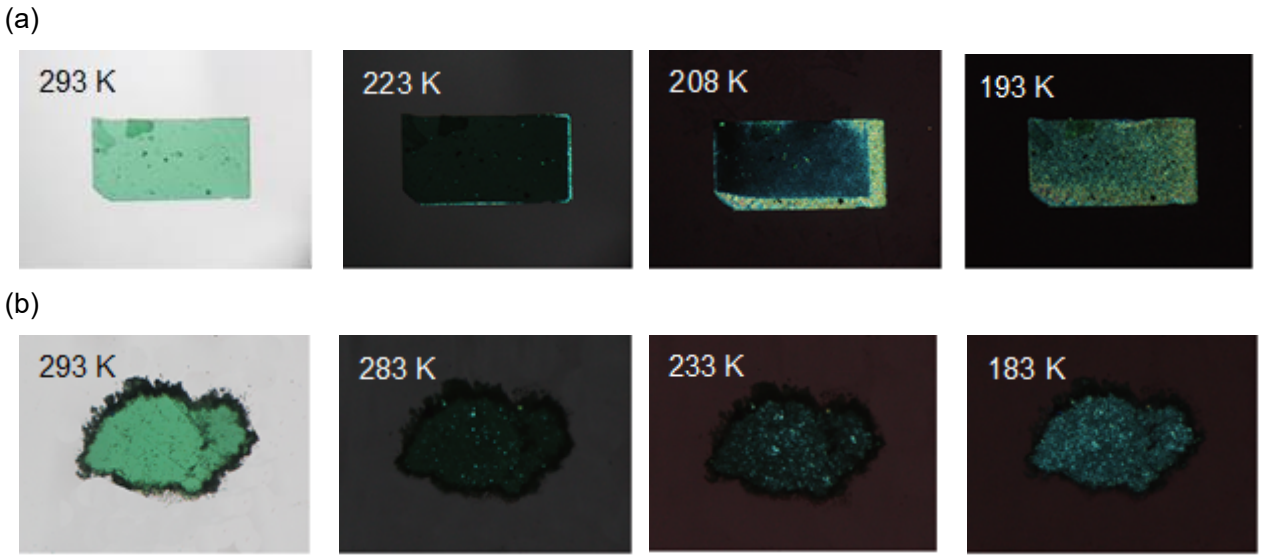

Figure S2. Polarized micrographs of [**2**][CF_3BF_3] that were taken during cooling: (a) Single crystal and (b) powder.

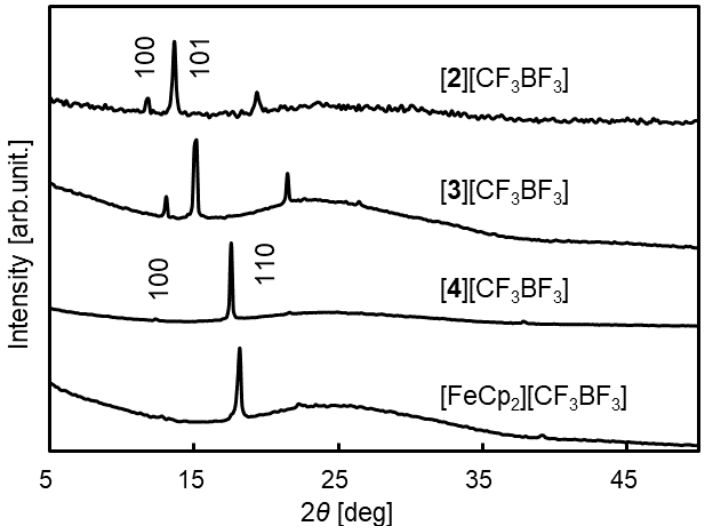

Figure S3. Powder X-ray diffraction patterns at 293 K (CuKα radiation),

(a) [**1**][CF_3BF_3]

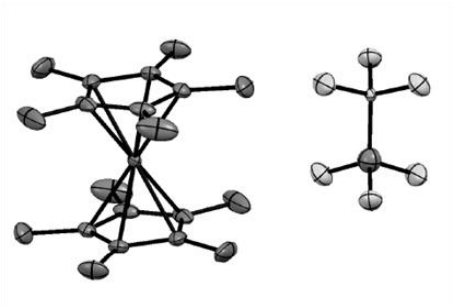

(b) [**1**][FSA]

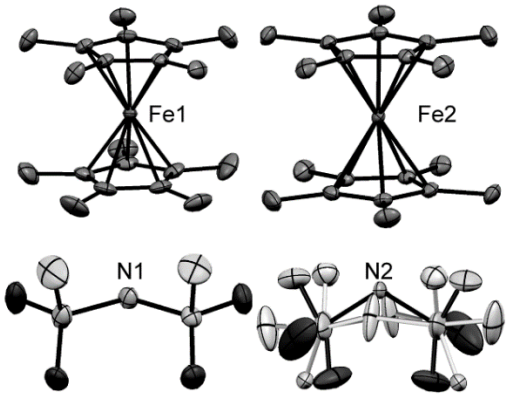

(c) [**1**][$B(CN)_4$]

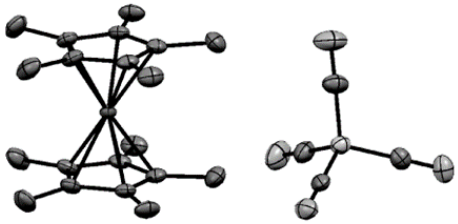

(d) [**1**][[$Co(C_2B_9H_{11})_2$]]

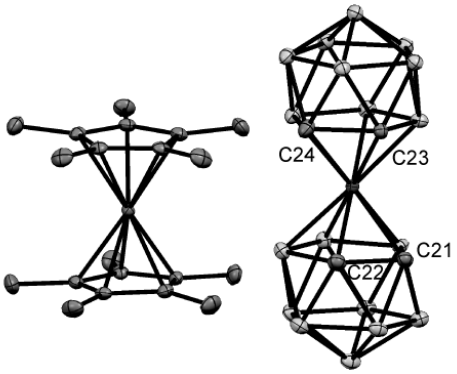

(e) [**1**]$_2$[$B_{12}F_{12}$]

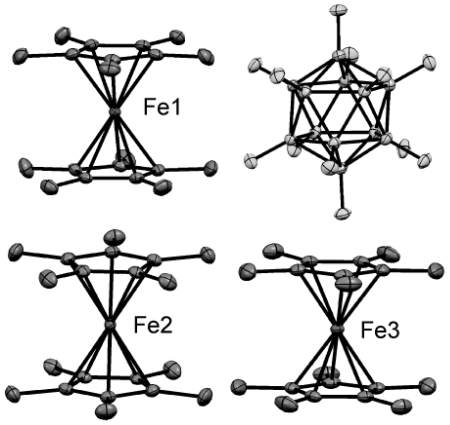

(f) [$FeCp_2$][OTf]

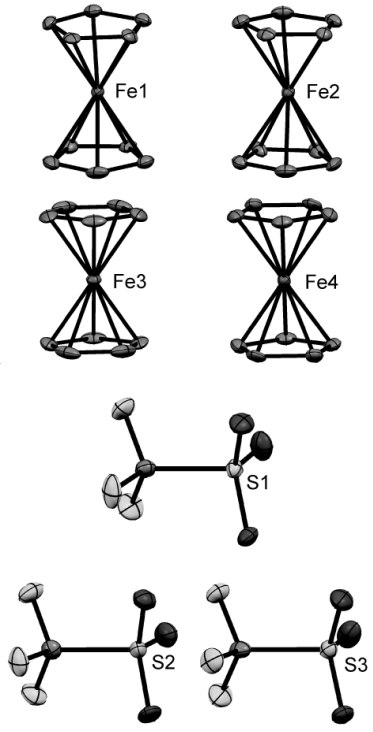

Figure S4. ORTEP drawings of the cations and anions. Hydrogen atoms have been omitted for clarity.

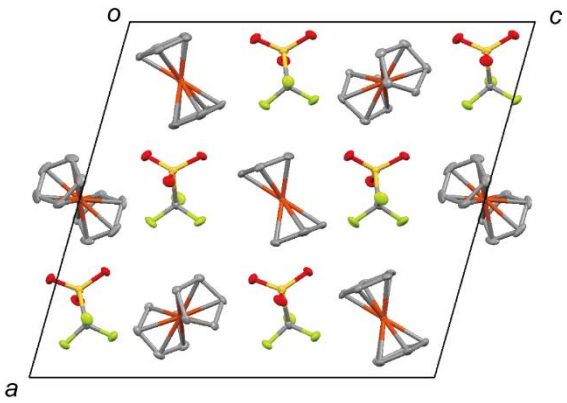

Figure S5. Packing diagram of [$FeCp_2$][OTf]. Hydrogen atoms have been omitted for clarity.

Table S1. Crystallographic parameters

	[**1**][CF_3BF_3]	[**1**][FSA]	[**1**][$B(CN)_4$]
Empirical formula	$C_{21}H_{30}BF_6Fe$	$C_{20}H_{30}F_2FeNO_4S_2$	$C_{24}H_{30}BFeN_4$
Formula weight	463.11	506.42	441.18
Crystal system	orthorhombic	monoclinic	trigonal
Space group	*P*nnm	*C*2/*c*	$P3_221$
a [Å]	8.6192(13)	30.3485(19)	9.7260(10)
b [Å]	9.7485(15)	12.2243(8)	9.7260(10)
c [Å]	12.6586(19)	18.8269(12)	22.601(2)
β [°]	90	102.5750(10)	90
V [Å^3]	1063.6(3)	6817.0(8)	1851.5(4)
Z	2	12	3
ρ_{calcd} [g cm^{-3}]	1.446	1.480	1.187
F(000)	482	3180	699
Temperature [K]	100	100	100
Reflns collected	5539	18883	10686
Independent reflns	1234	7458	2841
Parameters	82	460	143
R(int)	0.0230	0.0169	0.0312
R_1[a], R_w[b] ($I > 2\sigma$)	0.0261, 0.0658	0.0308, 0.0828	0.0205, 0.0568
R_1[a], R_w[b] (all data)	0.0270, 0.0661	0.0343, 0.0853	0.0208, 0.0571
Goodness of fit	1.095	1.081	1.062
$\Delta\rho_{max,min}$ [e Å^{-3}]	0.335, –0.251	0.644, –0.634	0.212, –0.361

[a] $R_1 = \Sigma||F_o| - |F_c|| / \Sigma|F_o|$. [b] $R_w = [\Sigma w (F_o^2 - F_c^2)^2 / \Sigma w (F_o^2)^2]^{1/2}$

Table S2. Crystallographic parameters

	[**1**][Co($C_2B_9H_{11}$)$_2$]	[**1**]$_2$[$B_{12}F_{12}$]	[$FeCp_2$][OTf]
Empirical formula	$C_{24}H_{52}B_{18}CoFe$	$C_{40}H_{60}B_{12}F_{12}Fe_2$	$C_{11}H_{10}F_3FeO_3S$
Formula weight	650.01	1010.30	335.10
Crystal system	monoclinic	monoclinic	monoclinic
Space group	$P2_1/n$	$P2_1/n$	$P2_1/c$
a [Å]	14.0677(9)	13.3674(17)	16.4200(11)
b [Å]	13.7291(9)	15.5063(19)	13.0629(9)
c [Å]	18.5367(12)	22.604(3)	17.6439(12)
β [°]	112.2270(10)	94.8470(10)	105.4730(10)
V [Å^3]	3314.1(4)	4668.6(10)	3647.3(4)
Z	4	4	12
ρ_{calcd} [g cm^{-3}]	1.303	1.437	1.831
F(000)	1356	2080	2028
Temperature [K]	100	100	90
Reflns collected	18472	25940	22433
Independent reflns	7275	10254	8058
Parameters	429	618	517
R(int)	0.0149	0.0167	0.0429
R_1[a], R_w[b] ($I > 2\sigma$)	0.0247, 0.0688	0.0270, 0.0751	0.0386, 0.0767
R_1[a], R_w[b] (all data)	0.0253, 0.0694	0.0281, 0.0762	0.0777, 0.0903
Goodness of fit	0.962	1.030	0.973
$\Delta\rho_{max,min}$ [e Å^{-3}]	0.461, –0.582	0.390, –0.358	0.378, –0.478

[a] $R_1 = \Sigma||F_o| - |F_c|| / \Sigma|F_o|$. [b] $R_w = [\Sigma w (F_o^2 - F_c^2)^2 / \Sigma w (F_o^2)^2]^{1/2}$